

Synthesis Of Efficient Calcium Silicate Catalyst For The Degradation Of Acridine Orange And Victoria Blue B Dyes

Santhosh, A.M., Yogendra, K., Mahadevan, K.M., Madhusudhana, N.

Abstract: Calcium Silicate nanoparticle was prepared using available calcium nitrate, silica fumes and fuel urea by solution combustion method. The prepared nanoparticles were characterized by XRD, SEM-EDAX, TEM and UV-Vis absorbance spectroscopy. The results of XRD revealed the presence of orthorhombic structure. The average size of prepared nanoparticles was found to be 13nm and the particle size less than 48nm confirmed by TEM. The optical band gap was found to be 4.6eV. The degradation efficacy was successfully examined for acridine orange and victoria blue B dye under sunlight. The degradation efficacy was achieved at 98.33% for acridine orange dye and 97.63% for victoria blue B dye in acidic pH.

Index Terms: Acridine Orange, Calcium Silicate, Characterization, Dyes, Degradation, Nanoparticles, Victoria Blue B

1 INTRODUCTION:

The industries are the major source for the water pollution. Textile, paper, rubber and plastic industries releases dye containing effluents and are responsible for major environmental pollution. The dyes, which are present in the effluents, are highly mutagenic, carcinogenic, non-biodegradable and colored pigments can cause severe damage to the surrounding living organisms [1], [2]. Therefore, the researchers have focused on the removal of dyes from wastewater. Several treatments methods have been experimented for the removal of dyes, such as adsorption, ozonization, reverse osmosis, and chemical oxidation. Conventional treatment methods such as absorption or coagulation are not efficiently removing the pollutants from wastewater. The partially degraded organic compounds are transferred one medium to another medium [3], [4]. Semiconductor photocatalysis another conventional treatment method and effectively removed the organic pollutants without producing any secondary pollutants by utilizing natural resources i.e., solar energy [5]. Various semiconductors photocatalysts such as, TiO₂, ZnO, CdS and ZnS [6] were used in the photocatalysis. These photocatalysts were cost-efficient, effective and eco-friendly, used to eliminate environmental problems. It is an effective method when compared to the other methods. Calcium silicate (CaSiO₃) commonly used material in ceramics, tiles, and cement manufacturing industries and having properties such as, low shrinkage, whiteness, lack of volatile constituents, good strength, fluxing characteristics, body permeability, and a circular shape [7]. It is widely used as bone filters, [8] drug delivery, bone tissue regeneration, [9] and also used as a host of phosphors and ceramic insulators [10]. Various methods for the synthesis of CaSiO₃ such as, solid state reaction, sol-gel, co-precipitation, combustion, [10] spray pyrolysis, hydrothermal, polymer pyrolysis, etc.[7].

In the present study, synthesized calcium silicate nanoparticle by solution combustion method (SCM) and characterized by XRD, SEM-EDAX, TEM and UV-Visible spectroscopic studies. This study focused on the photocatalytic activity of victoria blue B (VBB) and acridine orange dye (AO). VBB and AO dyes are widely used in fabrics such as wool, silk, nylon, acrylics, biological staining, printing and dyeing, leather, ink and lithography. These dyes cause some health effects such as, irritating effect on eyes and nose, respiratory system, skin dermatitis and mutagenic affects [11], [12], [13].

2 MATERIALS AND METHODS

2.1 SYNTHESIS AND CHARACTERIZATION OF NANOPARTICLES

Commercially available chemicals like calcium nitrate, urea (Hi-media Pvt. Ltd Mumbai) and silica fumes, victoria blue B and acridine orange dyes (Sigma Aldrich Pvt. Ltd Mumbai) were used without any purification. The chemical structure of VBB (λ_{max} 615nm) and AO (λ_{max} 492nm) dyes are represented in figure 1.

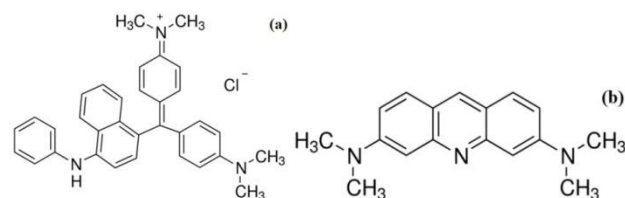


Figure 1: Chemical Structure of (a)VBB and (b) AO

The Stoichiometric mixture of calcium nitrate (7.08g), silica fumes (surface area 200 m²/g) (1.8g) and fuel urea (3.02g) was taken in a crucible and dissolved using double distilled water. The solution was placed in a preheated muffle furnace (600°C), after combustion process the obtained particles were finely crushed and used for characterization and photocatalytic activity. The propellant chemistry reaction is presented below.



- Department of P. G. Studies and Research in Environmental Science, Kuvempu University, Jnana sahyadri, Shankaraghatta, Shivamogga, Karnataka, INDIA
- Department of P. G Studies and Research in Chemistry, Kuvempu University,
- Jnana sahyadri, Shankaraghatta, Shivamogga, Karnataka, INDIA
- Corresponding Author: Yogendra K. e-mail: yogendraku@gmail.com, Tel +91-9448149461

Further, obtained nanoparticles were characterized by XRD (Make: Bruker AXS D8). Surface morphology and elemental analysis were measured by SEM-EDAX (Make: JEOL JSM - 6390LV). Further, crystal structure and size were analyzed during TEM (Make: JEOL JEM-2100) and optical band gap (OBG) determination was carried out using UV-visible spectrophotometer wavelength of 175 – 3300nm (Make: Varian, Cary 5000).

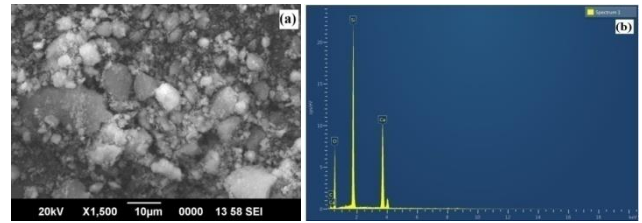


Fig. 3: (a) SEM (b) EDAX

2.2 EXPERIMENTAL PROCEDURE

The stock solution was prepared by dissolving 0.025g of VBB and 0.015g of AO dye in dye from stock solution was further diluted to 50 ml using double distilled water and pH was adjusted by adding NaOH or HCl. The experimental set up was placed on a magnetic stirrer under direct sunlight between 11am to 2pm (180 min). During the experiment, an aliquot of 5 mL was drawn out every 30 minutes to monitor the degradation process using UV-Visible spectrophotometer. All the experiments were conducted in 100ml beakers (Borosil), and to avoid evaporation of dye solution in sunlight, the beakers were covered by using petri plates. The percentage degradation was calculated following the methods of [14].

3 RESULT AND DISCUSSION

3.1 XRD

The synthesized calcium silicate nanoparticles are shown in Fig. 1. The obtained patterns of calcium silicate nanoparticles were confirm the presence of orthorhombic structure and well agreement with the JCPDS card number 01-087-1257. The particle size of CaSiO_3 nanoparticle was calculated by Scherer's formula (Eq. 2) and size of the CaSiO_3 was 13nm.

$$D = 0.94\lambda / \beta \cos\theta \quad (\text{Eq. 2})$$

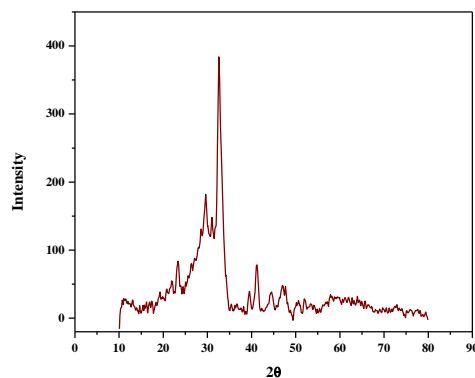


Fig. 1: XRD of synthesized calcium silicate nanoparticles

3.2 SEM AND EDAX

The surface morphology and elemental analysis of synthesized nanoparticle is shown in Fig. 3. Fig. 3a illustrated that, the enlarged images shows uneven distribution and particles are aggregated. Fig. 3b illustrated the presence of calcium silicate nanoparticles. The weight and atomic percentage was found to be O=45.84%, Ca=28.22%, Si=24.94% and O=60.26%, Ca=21.01% and Si=18.28% respectively.

3.3 TEM

The obtained TEM images of CaSiO_3 nanoparticles are shown in Fig 4. The surface morphology and size of CaSiO_3 nanoparticles were determined. The particle sizes vary from 20nm to 48nm shown in Fig. 4b and the surface of the catalyst looks like non-homogenous and agglomerated. Further, d-space value is calculated from the distance between the two bright hotspots found to be 7.60nm. The d-space value was found to be 0.26nm.

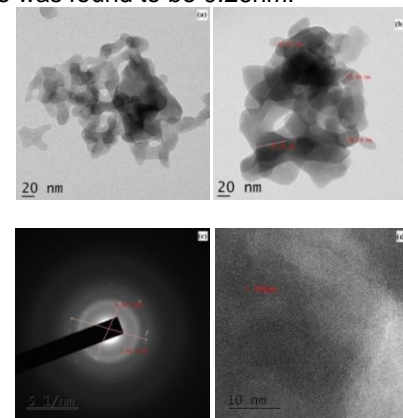


Fig. 4: TEM micrographs of CaSiO_3 nanoparticles (a) TEM image (b) HR-TEM image (c) SAED Patterns (d) lattice fringes

3.3 UV-VISIBLE ABSORPTION SPECTRUM

The spectrum of prepared CaSiO_3 nanoparticle is shown in figure 5. The OBG of CaSiO_3 nanoparticle is calculated from the Tauc relation (Eq. 4). The OBG of prepared nanoparticle was found to be 4.6eV

$$(\alpha h\nu) \sim (h\nu - E_g)^{1/2} \quad (\text{Eq. 3})$$

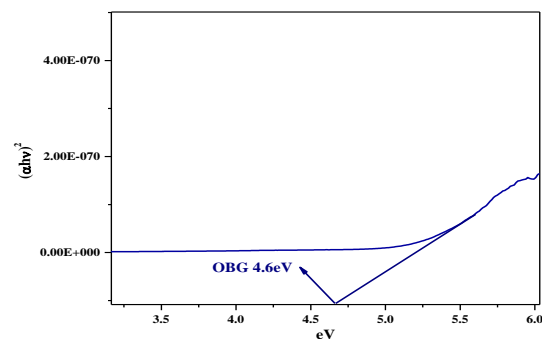


Fig. 5: Optical Band Gap of CaSiO_3 nanoparticles

3.4 EFFECT OF CATALYST CONCENTRATION

To evaluate the CaSiO_3 concentration for the removal of AO and VBB dyes varied from 0.020g to 0.060g was studied with constant dye concentration (1×10^{-4} mol/dm³) in a

neutral condition. The percentage of degradation efficacy increases with increase in CaSiO_3 loading up to 0.040g for AO and 0.050g for VBB dyes. Where, the maximum degradation achieved 95.97% at 0.040g for AO dye and VBB dye achieved 94.01% at 0.050g in 180min shown in Fig. 6. Below the optimum CaSiO_3 concentration the degradation decreases due to lack of availability of active surface area for the degradation of AO and VBB dyes. Further increase in the degradation efficacy due to availability more reactive sites of the catalyst, which initiates the degradation reaction by generating hydroxyl and superoxide radicals [15], [16]. The degradation efficacy of AO and VBB dyes at higher CaSiO_3 concentration (0.040g for AO and 0.050g for VBB) decreases due to reflectance of light by CaSiO_3 particles and decreases the active surface area due to agglomeration [17], [18].

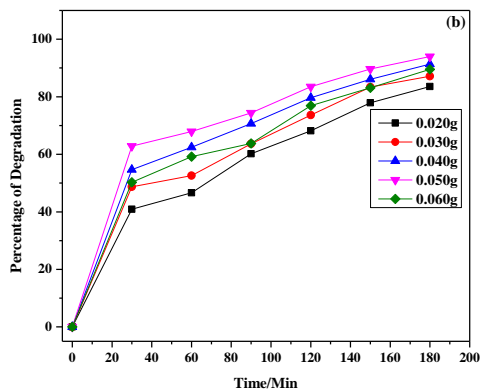
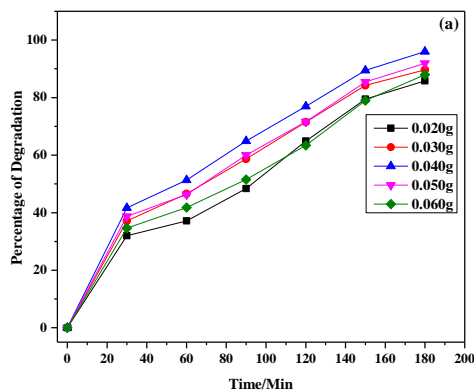


Fig. 6: Catalyst Concentration (a) AO (b) VBB

3.5 EFFECT OF PH

pH plays a major role in the degradation of dyes, which affects the adsorbent capacity for the elimination of adsorbent. pH varied from 2-10 for the degradation of AO and VBB dyes with constant catalyst concentration (0.040g for AO and 0.050g for VBB) and dye concentration (1×10^{-4} mol/dm³). The degradation efficacy of AO (Fig.7a) dye increased from 90.47% to 93.3% from pH 2 to 4 and decreased to 74.32% at pH 10 in 180 min and for VBB (Fig. 7b) dye increases from 88.02% to 97.63% from pH 2 to 6 and decreased to 90.73% at pH 10 in 180 min. The optimum pH achieved at pH 4 for AO and pH 6 for VBB dyes. However, the degradation shows efficient in acidic

medium compared to basic medium. In acidic medium, the formation of OH^- ions and competition of OH^- ions and the dyes for occupying the adsorption sites on the CaSiO_3 nanoparticles favours the degradation of the dyes and also a large number of O_2 is reduced into $\cdot\text{O}_2^-$ radicals by photoelectrons [1], [19]. In the basic pH condition, the particles are negatively charged and affect the interaction of molecules. The competence of hydroxyl radicals tend to adsorb on the surface of the catalyst are rapidly scavenged and the probability of catalyst reacts with dyes are very low [20], [21], [22], [23], [24]. Hence, the degradation efficacy decreased.

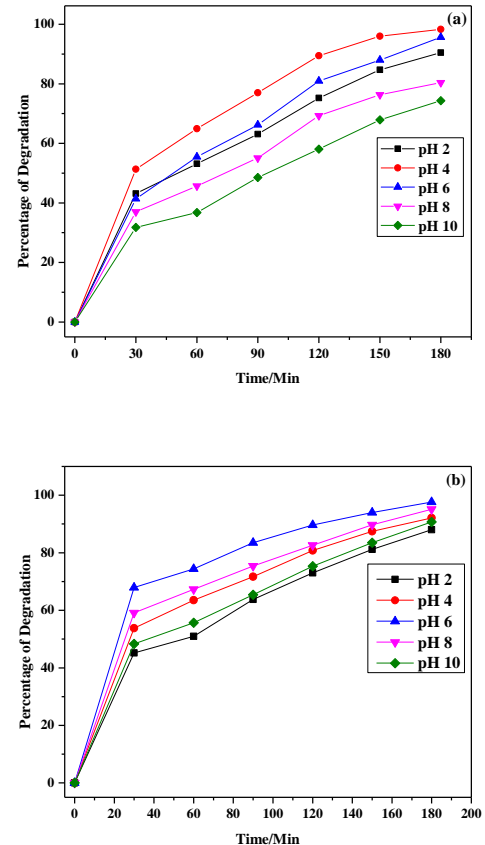


Fig. 7: pH (a) AO (b) VBB

3.6 EFFECT OF DYE CONCENTRATION

The treatment of wastewater disposed after finishing the dyeing process from the industries having different dye concentration. The intensity of the colour affects the reaction media, the dye concentration was varied from 1×10^{-4} mol/dm³ to 4×10^{-4} mol/dm³ while keeping constant pH and CaSiO_3 concentration for AO (0.040g/pH 4/50ml) and VBB (0.050g/pH 6/50ml) dyes as shown in Fig.8. The obtained result for AO dye is 98.33% at 1×10^{-4} mol/dm³, 90.03% at 2×10^{-4} mol/dm³, 82.41% at 3×10^{-4} mol/dm³ and 75.20% at 4×10^{-4} mol/dm³. VBB dye achieved 97.63% at 1×10^{-4} mol/dm³, 88.60% at 2×10^{-4} mol/dm³, 80.01% at 3×10^{-4} mol/dm³ and 74.83% at 4×10^{-4} mol/dm³ respectively. Experimental results illustrated that, the percentage of degradation gradually decreases with increase in dye concentration. At higher dye concentration less adsorption of dye molecules on the CaSiO_3 surface which directly affects to lack of availability of active surface area [17], [25].

Above the $2 \times 10^{-4} \text{ mol/dm}^3$ dye concentration, the percentage of degradation decreased due to less photons entering into the solution, which results in the decrease in formation of hydroxyl radicals and suppress the degradation reaction [15], [26], [27], [28], [29].

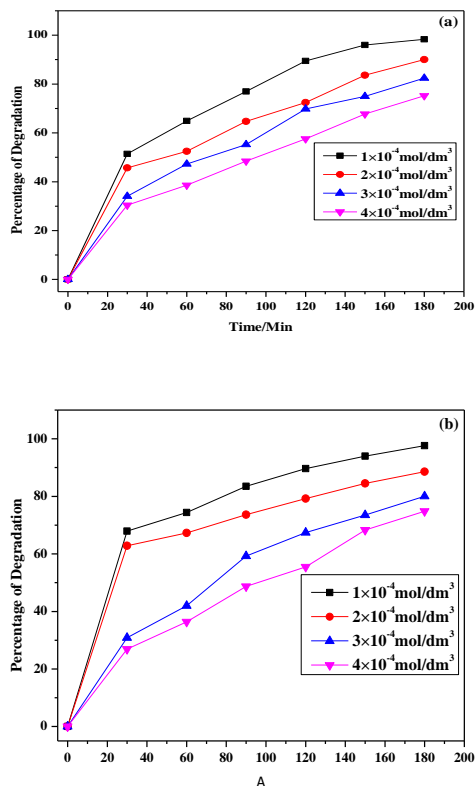


Fig. 8: Dye Concentration (a) AO (b) VBB

4 CONCLUSION

Calcium Silicate nanoparticle was successfully synthesized by solution combustion method and characterized by XRD, SEM-EDAX, TEM, and also determined the optical band gap. The average particle size was found to be 13nm confirmed by XRD studies and EDAX revealed the presence of Ca, Si, and O. SEM and TEM images showed the surface morphology of the nanoparticles and TEM confirmed the presence of micro-pores (particles size less than 2 nm). The AO and VBB dyes were selected for the photocatalytic degradation. The maximum degradation was achieved at 98.33% at 0.040g/pH 4/ $1 \times 10^{-4} \text{ mol/dm}^3$ for acridine orange dye and 97.63% at 0.050g/pH 6/ $1 \times 10^{-4} \text{ mol/dm}^3$ for victoria blue B dye. The AO dye showed efficient degradation when compared to VBB dye. The usage of CaSiO_3 nanoparticle in the treatment of wastewater is found to be efficient and desirable.

ACKNOWLEDGEMENTS

The authors would like to acknowledge SAIF, Cochin University, Cochin, for providing necessary facilities.

REFERENCES

[1]. X. Chen, Z. Wu, D. Liu, and Z. Gao, "Preparation of ZnO Photocatalyst for the Efficient and Rapid

Photocatalytic Degradation of Azo Dyes," *Nanoscale Research Letters*, Vol. 12, no. 143, pp. 1-10, 2017, doi: 10.1186/s11671-017-1904-4.

- [2]. Y. Chiu, T.M. Chang, C. Chen, M. Sone, and Y. Hsu, "Mechanistic Insights into Photodegradation of Organic Dyes Using Heterostructure Photocatalysts," *Catalysts*, Vol. 9, no. 430, pp. 1-32, 2019, doi:10.3390/catal9050430.
- [3]. M. Bagheri, N.R. Najafabadi, and E. Borna, "Removal of reactive blue 203 dye photocatalytic using ZnO nanoparticles stabilized on functionalized MWCNTs," *Journal of King Saud University Science*, Vol. 32, pp. 799-804, 2020, doi.org/10.1016/j.jksus.2019.02.012.
- [4]. Z. Durmus, B.Z. Kurt, and A. Durmus, "Synthesis and Characterization of Graphene Oxide/Zinc Oxide (GO/ZnO) Nanocomposite and Its Utilization for Photocatalytic Degradation of Basic Fuchsin Dye," *Chemistry Select*, Vol. 4, pp. 271-278, 2019, doi: 10.1002/slct.201803635.
- [5]. Y. Jiang, Y. Sun, H. Liu, F. Zhu, and H. Yin, "Solar photocatalytic decolorization of C.I. Basic Blue 41 in an aqueous suspension of TiO_2 -ZnO," *Dyes and Pigments*, Vol. 78, pp. 77-83, 2008, doi:10.1016/j.dyepig.2007.10.009.
- [6]. A. Gnanaprakasam, V.M. Sivakumar, P.L. Sivayogavalli, and M. Thirumarimurugan, "Characterization of TiO_2 and ZnO nanoparticles and their applications in photocatalytic degradation of azo dyes," *Ecotoxicology and Environmental Safety*, Vol. 121, pp. 121-125, 2015, doi.org/10.1016/j.ecoenv.2015.04.043.
- [7]. J. Palaniraja, P. Arunachalam, U. Vijayalakshmi, M.A. Ghanem, and S.M. Roopan, "Synthesis of calcium silicate nanoparticles and its catalytic application in Friedlander reaction," *Inorganic and Nano-Metal Chemistry*, Vol. 47, no. 6, pp. 946-949, 2017, doi.org/10.1080/24701556.2016.1241274.
- [8]. M. Mabrouk, S.A. ElShebiney, S.H. Kenawy, G.T. El-Bassyouni, and E.M. Hamzawy, "Novel, Cost-effective, Cu-doped Calcium Silicate Nanoparticles for bone Fracture Intervention: Inherent Bioactivity and in Vivo performance," *Journal of Biomedical Material Research Part-B*, Vol. 107, no. 2, pp. 1-12, 2018, doi.org/10.1002/jbm.b.34130.
- [9]. S.M. Li, N. Jia, J.F. Zhu, M.G. Maa, and R.C. Sun, "Synthesis of cellulose-calcium silicate nanocomposites in ethanol/water mixed solvents and their characterization," *Carbohydrate Polymers*, Vol. 80, pp. 270-275, 2010, doi:10.1016/j.carbpol.2009.11.024.
- [10]. S.P. Singh, and B. Karmakar, "Mechanochemical Synthesis of Nano Calcium Silicates particles at Room Temperatures," *New journal of Glass and Ceramics*, Vol. 1, pp. 21-25, 2011, doi:10.4236/njgc.2011.12005.
- [11]. G.R. Chaudhary, P. Saharan, A. Umar, S.K. Mehta, and S. Mor, "Well-Crystalline ZnO Nanostructures for the Removal of Acridine Orange and Coomassie Brilliant Blue R-250 Hazardous Dyes," *Science of Advanced Materials*, Vol. 5, pp. 1886-1894, 2013, doi.org/10.1166/sam.2013.1701.
- [12]. B. Pare1, P. Singh, and S.B. Jonnalgadda, "Degradation and mineralization of Victoria blue B dye in a slurry photoreactor using advanced oxidation

- process,” *Journal of Scientific & Industrial Research*, Vol. 68, pp. 724-729, 2009.
- [13]. M. Yadav, S. Ali, and O.P. Yadav, “Photo-catalytic Degradation of Victoria Blue-B Dye using ZnS and Ag-N co-doped ZnS Nanoparticles under Visible Radiation,” *Journal of Applicable Chemistry*, Vol. 3, no. 6, pp. 2563–2572, 2014.
- [14]. H.R. Pouretedal, A. Norozi, M.H. Keshavarz, and A. Semnani, “Nanoparticles of zinc sulfide doped with manganese, nickel and copper as nanophotocatalyst in the degradation of organic dyes,” *Journal of Hazardous Materials*, Vol. 162, no. 2–3, pp. 674–681, 2009, doi.org/10.1016/j.jhazmat.2008.05.128.
- [15]. M.H. Abdellah, S.A. Nosier, A.H. El-Shazly, and A.A. Mubarak, “Photocatalytic decolorization of methylene blue using TiO₂/UV system enhanced by air sparging,” *Alexandria Engineering Journal*, Vol. 57, pp. 3727–3735, 2018, doi.org/10.1016/j.aej.2018.07.018.
- [16]. G. Shilpa, K. Yogendra, K.M. Mahadevan, and A.M. Santhosh, “Photocatalytic Degradation of Mono Azo Dye Acid Red 88 by using Synthesized Calcium Aluminate Nanoparticle and its Kinetics,” *Research Journal of Chemistry and Environment*, Vol. 23, no. 10, pp. 29-35, 2019.
- [17]. S. Karuppaiah, R. Annamalai, A. Muthuraj, S. Kesavan, R. Palani, S. Ponnusamy, E.R. Nagarajan, and S. Meenakshisundarama, “Efficient photocatalytic degradation of ciprofloxacin and bisphenol A under visible light using Gd₂WO₆ loaded ZnO/bentonite nanocomposite,” *Applied Surface Science*, Vol. 481, pp. 1109–1119, 2019, doi.org/10.1016/j.apsusc.2019.03.178.
- [18]. A. Raja, P. Rajasekaran, K. Selvakumar, M. Arunpandian, K. Kaviyarasu, S.A. Bahadura, and M. Swaminathan, “Visible active reduced graphene oxide-BiVO₄-ZnO ternary photocatalyst for efficient removal of ciprofloxacin,” *Separation and Purification Technology*, Vol. 233, pp. 1-11, 2020, doi.org/10.1016/j.seppur.2019.115996.
- [19]. A.M. Santhosh, K. Yogendra, K.M. Mahadevan, I.H. Mallikarjuna, and N. Madhusudhana, “Application of Nickel Calcite Nanoparticles in the Photodegradation of direct green 6 Dye,” *International Research Journal of Environmental Sciences*, Vol. 7, no. 6, pp. 12-18, 2018.
- [20]. G. Kale, S. Arbuji, U. Kawade, S. Kadam, K. Nikam, B. Kale, “Paper templated synthesis of nanostructured Cu–ZnO and its enhanced photocatalytic activity under sunlight.” *Journal of Materials Science: Materials in Electronics*, Vol. 30, pp. 7031–7042, 2019, doi.org/10.1007/s10854-019-01020-w.
- [21]. S.B. Patil, T.N. Ravishankar, K. Lingaraju, G.K. Raghu, and G. Nagaraju, “Multiple applications of combustion derived nickel oxide nanoparticles,” *Journal of Materials Science: Materials in Electronics*, Vol. 29, pp. 277–287, 2018, doi:10.1007/s10854-017-7914-2.
- [22]. N. Saikumari, Y. Preethi, B. Abarna, and G.R. Rajarajeswari, “Ecofriendly, green tea extract directed sol–gel synthesis of nano titania for photocatalytic application,” *Journal of Materials Science: Materials in Electronics*, Vol. 30, pp. 6820–6831, 2019, doi.org/10.1007/s10854-019-00994-x.
- [23]. M.E. Villanueva, G.J. Copello, and V.C. Dall-Orto, “Solar light efficient photocatalytic activity degradation of emergent contaminants by coated TiO₂ nanoparticles,” *New J. Chem.*, Vol. 42, pp. 15405-15412, 2018, doi: 10.1039/c8nj02332h.
- [24]. M.N. Zafar, Q. Dar, F. Nawaz, M.N. Zafar, M. Iqbal, and M.F. Nazar, “Effective adsorptive removal of azo dyes over spherical ZnO nanoparticles,” *Journal of Materials Research and Technology*, Vol. 8, no. 1, pp. 713–725, 2019, doi.org/10.1016/j.jmrt.2018.06.002.
- [25]. A.M. Santhosh, K. Yogendra, K.M. Mahadevan, I.H. Mallikarjuna, and N. Madhusudhana, “Efficiency of Photodegradation Properties of Nickel Calcite Nanoparticle Synthesized by solution combustion method,” *International Journal of Scientific Research in Physics and Applied Sciences*, Vol. 6, no. 5, pp. 48-56, 2018.
- [26]. J. Duraimurugan, G.S. Kumar, P. Maadeswaran, S. Shanavas, P.M. Anbarasan, and V. Vasudevan, “Structural, optical and photocatalytic properties of zinc oxide nanoparticles obtained by simple plant extract mediated synthesis,” *Journal of Materials Science: Materials in Electronics*, Vol. 30, pp. 1927-1935, 2019, doi.org/10.1007/s10854-018-0466-2.
- [27]. S. Farhadi, F. Manteghi, and R. Tondfekr, Removal of Congo red by two new zirconium metal–organic frameworks: kinetics and isotherm study,” *Monatshefte für Chemie-Chemical Monthly*, Vol. 150, pp. 193–205, 2019, doi.org/10.1007/s00706-018-2329-1.
- [28]. A. Nasiri, F. Tamaddon, M.H. Mosslemin, M.A. Gharaghani, and A. Asadipour, “New magnetic nanobiocomposite CoFe₂O₄@methycellulose: facile synthesis, characterization, and photocatalytic degradation of metronidazole,” *J Mater Sci: Mater Electron*, Vol. 30, pp. 8595-8610, 2019, doi.org/10.1007/s10854-019-01182-7.
- [29]. H. Sudrajat, and S. Babel, “Comparison and mechanism of photocatalytic activities of N-ZnO and N-ZrO₂ for the degradation of rhodamine 6G,” *Environ Sci Pollut Res*, Vol. 23, pp. 10177-10188, 2016, doi:10.1007/s11356
- [30]. -016-6191-6.